Bergische Universität Wuppertal

Fakultät für Mathematik und Naturwissenschaften

Institute of Mathematical Modelling, Analysis and Computational Mathematics (IMACM)

Preprint BUW-IMACM 26/14

Daniel Walsken, Matthias Ehrhardt and Pavel Petrov

A perfectly matched layer approach for the spectral split-step Padé method

July 3, 2026

http://www.imacm.uni-wuppertal.de

A PERFECTLY MATCHED LAYER APPROACH FOR THE SPECTRAL SPLIT-STEP PADÉ METHOD*

DANIEL WALSKEN†, MATTHIAS EHRHARDT†,‡, AND PAVEL PETROV§

Abstract. The split-step-Padé (SSP) method is widely used to model wave phenomena in various applications, including radio physics, optics and acoustics. In this method, the propagator of the one-way counterpart of the Helmholtz equation is computed through its Padé approximant and a finite-difference discretization of the transverse operator. This work develops and validates numerically a spectral counterpart of the SSP method. A key challenge in practical applications is inverting the transverse operator in the presence of perfectly matched layers (PMLs), which are commonly used to truncate the computational domain. Such inversion can be accomplished using Krylov subspace methods, which converge rapidly, provided that a suitable preconditioner is used. We also study the analytical properties of the spectral SSP marching scheme under periodicity conditions in the transverse variable. We validate the newly developed spectral SSP method numerically in two realistic test scenarios from radio physics and underwater acoustics.

Key words. Split-Step Padé method, Perfectly Matched Layer, Krylov method, wide-angle parabolic equation, Spectral discretization

MSC codes. 68Q25, 68R10, 68U05

Introduction. The propagation of waves in inhomogeneous media is a fundamental problem in applied mathematics and computational physics. It has numerous applications in optics, radio physics, underwater and atmosphere acoustics, and geophysical exploration. The governing model is usually the Helmholtz equation, whose direct numerical solution in large or unbounded domains is computationally expensive due highly oscillatory nature of its solutions that imposes severe discretization step restriction. A common approach to reducing computational complexity is to use parabolic approximations of the Helmholtz equation, which were first introduced by Leontovich and Fock [29, 55]. These models transform the original boundary value problem into an initial value problem in a preferred propagation direction, thereby significantly reducing computational effort. Although such reformulation neglects back-scattered waves, it has proven to be extremely efficient in many applications, where parabolic equations have become main computational tools [12, 26, 30, 38], especially after the introduction of *split-step Fourier* (SSF) spectral solvers (mostly for narrow-angle parabolic equations).

However, classical parabolic equation methods are limited in their ability to accurately capture wide-angle propagation effects. This limitation has been overcome by the development of *wide-angle parabolic equations* (WAPEs), which approximate the square-root operator arising from the factorization of the Helmholtz operator using rational Padé approximants [1, 12, 13, 26, 30, 45]. It is important that WAPEs substantially improve angular accuracy while preserving computational efficiency paraxial equations. The next major improvement of WAPEs was the invention of the *split-step Padé* (SSP) method [5, 13] that aims at approximating the *propagator* of the operator square root (i.e., the exponential that emerges from integration of one-way Helmholtz equation over small step), by a Padé series. This has proven to be much more effi-

*Submitted to the editors June 30, 2026.

†Applied and Computational Mathematics, University of Wuppertal, Wuppertal, Germany (walsken@uni-wuppertal.de, ehrhardt@uni-wuppertal.de).

‡Corresponding author.

§Instituto de Matemática Pura e Aplicada, Rio de Janeiro, Brazil (pavel.petrov@impa.br).

cient than approximating the square-root operator itself, both in terms of accuracy and computational efficiency. A particularly impressive fact about SSP method is that in can be used with integration step of about 10 wavelengths [13, 43]. Classical SSP methods are widely used in many areas such as optics, acoustics and radio physics (both for solving direct and inverse problems) where they are often considered a huge improvement as compared to SSF/WAPE [37, 38, 14, 32, 39, 41, 42, 57, 40].

Recently, it was shown that the advantages of the SSF and SSP methods could be combined by computing Padé approximants at each step of the marching scheme via the fast Fourier transform (FFT) [56]. Because they are more accurate for smooth solutions, spectral methods are a good choice for solving parabolic wave equations numerically [10, 20]. In particular, Fourier-based discretizations yield spectral (often exponential) convergence and can be efficiently implemented using FFTs [51].

A central challenge in the numerical treatment of wave propagation problems is the modeling of unbounded domains [21, 24, 47, 53]. Truncating the computational domain generally leads to artificial reflections at the boundaries, which can spoil the numerical solution due to non-physical reflections at the artificial boundaries.

Among the various approaches developed to address this issue, *perfectly matched layers* (PML), introduced by Bérenger [8], have proven to be particularly effective. PML involves surrounding the computational domain with an artificial absorbing layer obtained via complex coordinate stretching, which leads to exponential attenuation of outgoing waves without reflection at the artificial boundary. PML techniques have been extensively studied for various wave propagation models, including the Helmholtz and Maxwell equations [11, 25, 34] Their mathematical properties, such as well-posedness, stability, and convergence, have been analyzed in several works, including [4, 7, 27]. However, incorporating PML techniques into split-step Padé methods in combination with spectral discretizations is considerably less developed, although several important ideas have been recently proposed [2, 3].

In the spectral SSP framework, introducing a PML leads to additional analytical and numerical challenges. In particular, the complex coordinate stretching destroys the simple diagonal structure of the differential operator in Fourier space, which is essential for efficient inversion in the classical spectral setting. Consequently, the resulting operators cannot be inverted analytically in Fourier space, therefore iterative methods, such as Krylov subspace solvers (e.g., GMRES [46, 52]), must be employed. This raises important questions regarding stability, efficiency, and the design of suitable preconditioners.

The goal of this work is to develop and analyze a *spectral split-step Padé* (SSSP) method with a PML to efficiently solve mode parabolic equations. This approach combines a Fourier spectral discretization in the transverse direction and a Padé approximation of the propagator to achieve wide-angle capabilities. It also uses a PML formulation to treat unbounded domains within a finite computational region. Particular focus is placed on efficiently realizing the method numerically, including using Krylov subspace methods and constructing effective preconditioners based on operator splitting ideas.

From a mathematical perspective, recent advances have provided a rigorous analytical foundation for these approaches. In particular, the square-root operator appearing in parabolic wave equations has been studied within the framework of pseudodifferential operators, and the well-posedness of the associated evolution equations has been established in [18]. These results justify the use of exponential propagators and their rational approximations within the SSP framework.

We establish the stability and convergence properties of the proposed scheme.

Specifically, we analyze the dissipativity of the PML-modified operator, prove the stability of the Padé-based marching scheme, and derive a global error estimate combining contributions from the temporal discretization, spectral approximation in space, and PML layer truncation. These results rigorously justify the method and clarify the interplay between the different approximation components. We demonstrate the performance of the proposed method on benchmark problems from underwater acoustics, including flat-bottom and wedge configurations. We also apply the method to radio wave propagation in the atmosphere. The numerical results demonstrate that the method achieves high accuracy, even on relatively coarse grids. This highlights the effectiveness of the spectral discretization and the robustness of the PML formulation.

The remainder of the paper is organized as follows. Sections 1 and 2 introduce the mode parabolic equation and the spectral split-step Padé method in more detail. Section 3 presents the PML formulation and its incorporation into the spectral framework. Section 3 is devoted to the analytical properties of the method, including stability and convergence. Section 4 describes the application to radiowave propagation in the troposphere, and Section 5 deals with sound propagation in a 3D shallow-water waveguide. Finally, Section 6 provides concluding remarks.

1. The Split-Step Padé method. The *split-step Padé* (SSP) method was proposed to numerically integrate a one-way counterpart of Helmholtz-type elliptic equations. For the sake of clarity, we will write this equation as

$$\partial_x^2 U + \partial_y^2 U + k^2 U = 0\,, \tag{1.1}$$

where $U = U(x, y)$ is the wavefield, and $k = k(x, y)$ is the medium wave number. The physical meaning of U and k depends on the area of application, e.g., it can be transverse component of the electric field in a radiowave propagating in the troposphere or the amplitude of a vertical mode in the normal mode decomposition of the acoustic field (these two examples are considered in Section 4 and Section 5).

The following one-way counterpart of (1.1) can be obtained by a formal factorization of the Helmholtz operator and by retaining only the waves propagating in the positive direction of the x axis:

$$\partial_x U(x, y) = \mathrm{i}\sqrt{\partial_y^2 + k^2(x, y)}\, U(x, y)\,, \quad x, y \in [0, R] \times (-\infty, \infty)\,. \tag{1.2}$$

A mathematically rigorous definition of the square root of an operator for the case when its numerical range is bounded away from the real axis from above (this is always the case in real-world problems, as k has a positive imaginary part due to the medium attenuation) is given in [18] together with the existence and uniqueness proof for the initial-value problem for (1.2) in the half-space $x \geq 0$.

There are several reasons why one-way approximations Helmholtz-type equations are generally more practical than the latter. In particular, and important advantage from the viewpoint of scientific computing consists in the fact that a boundary-value problem for an elliptic equation is transformed into a a Cauchy problem for an evolutionary equation that can be integrated numerically by a marching scheme.

Another advantage is that the rapidly oscillating term $\mathrm{e}^{\mathrm{i}k_0 x}$ (the principal oscillation) in the propagation direction x defined by the reference wave number k_0 can be canceled out by introducing a new unknown function $u(x, y) = \mathrm{e}^{-\mathrm{i}k_0 x} U(x, y)$. Introducing the operator $\mathcal{X} = (\partial_y^2 + k_0^2 - k^2)/k_0^2$, we can write an equation for u as

$$\partial_x u(x, y) = \mathrm{i}k_0\big(\sqrt{1 + \mathcal{X}} - 1\big)u\,. \tag{1.3}$$

The solution of the latter equation can be computed by a marching scheme obtained by formally integrating it along a small interval of length h in x direction, i.e.,

$$u(x+h,y) = \exp\Big(\mathrm{i}k_0 h\big(\sqrt{1+\mathcal{X}}-1\big)\Big)u(x,y) = f(\mathcal{X})u(x,y)\,, \tag{1.4}$$

where $f(z) = \mathrm{e}^{\mathrm{i}t(\sqrt{1+z}-1)}$ is defined as a scalar function of a complex variable, and $t = k_0 h$. The exponential on the right-hand side of (1.4) is called *a propagator*.

The *Split-Step Padé (SSP) method* consists in the approximation of the pseudo-differential operator on the right-hand side of (1.4) by the $[P|P]$ Padé approximant R_P of the form

$$u(x+h,y) \approx R_P(\mathcal{X})u(x,y) = \left(d_0 + \sum_{j=1}^{P} \frac{d_j}{1+b_j\mathcal{X}}\right)u(x,y) = \left(d_0 u + \sum_{j=1}^{P} d_j w_j\right), \tag{1.5}$$

where the auxiliary functions w_j are calculated at each marching step in x by solving the following equations

$$(1+b_j\mathcal{X})w_j(y) = u(x,y)\,, \quad y\in(-\infty,\infty), \quad j = 1,2,\dots,P. \tag{1.6}$$

Over the years, numerous distinct varieties and extensions of the SSP framework have been proposed in order to adapt to more demanding physical scenarios. Examples include the high-order pseudo-differential developments by Antoine et al. [2], the multi-dimensional and electromagnetic wide-angle adaptations by Lu [36], the energy-conserving and reciprocity-preserving one-way wave formulations of Godin [22], and the vector/coupled-mode extensions in curvilinear domains by Petrov et al. [42].

Remark 1.1 (Computation of Padé coefficients). In this work, the coefficients of the Padé approximant are computed using the classical matrix method. This method involves solving the linear system associated with matching the Taylor coefficients of the propagator. While this approach is straightforward and widely used, it is well known that computing Padé approximants can lead to numerical ill-conditioning, particularly for higher approximation orders. Convergence and stability issues are discussed in detail in [17, Section III].

Several more robust alternatives have been proposed in the literature. In particular, Chebyshev-Padé techniques combine rational approximation with Chebyshev expansions to provide improved numerical behavior [16, Section 9.1.]. Furthermore, singular value decomposition (SVD)-based approaches can substantially improve robustness by mitigating the effects of nearly singular systems and eliminating spurious pole-zero pairs (Froissart doublets), see [23].

From a theoretical perspective, the convergence behavior of Padé approximants is closely related to fundamental questions in rational approximation theory. One of the most prominent examples is the Baker-Gammel-Wills conjecture, which concerns the convergence of diagonal Padé approximants to analytic functions. Although the conjecture is known to be false in full generality, it has motivated extensive research on the localization of poles and the convergence properties of Padé sequences. Since the SSP method relies on comparatively low approximation orders, the classical matrix method was sufficient for all numerical experiments reported in this paper.

In particular, numerical instabilities may manifest as spurious poles, the location of which can significantly impact the stability of the resulting rational propagator, cf. Section 3.1 and in particular Conjecture 3.3.

The above formulation provides an efficient forward propagation scheme. However, in this basic form, the treatment of unbounded domains remains an open issue. In Subsection 1.1, we introduce a *perfectly matched layer* (PML) to avoid artificial reflections at the boundaries. This work follows the notation of Antoine et al. [2].

Note that the proper definition of the square root $\sqrt{\partial_y^2 + k^2}$, let alone the mathematical properties of (1.2), is non-trivial. A rigorous definition of such operators and existence, uniqueness, and well-posedness for equations of the form (1.2) were established in a recent paper [18].

1.1. Perfectly Matched Layer. In wave propagation, a common computational problem is that the wave field on an unbounded, open domain Ω_{open} has to satisfy the Sommerfeld radiation boundary condition [49].

One of the more recent and computationally simplest methods is the introduction of a *perfectly matched layer* (PML), developed by Berénger [8] and applied to a parabolic wave equation by Levy [31]. The eponymous PML is a buffer domain Ω_{PML} around the truncated (physical) domain Ω_{Phys}, in which the physical coordinates are stretched and the field is dampened. In Cartesian coordinates for the simple case of a one-dimensional, symmetric domain of interest, this involves truncating the open domain $\Omega_{\text{open}} \supset \Omega_{\text{Phys}} = [-L_y^*, L_y^*]$ and introducing a layer $\Omega_{\text{PML}} = [-L_y, -L_y^*] \cup [L_y^*, L_y]$ around the physical domain (the domain of interest). The problem is then numerically solved on the computational domain $\Omega_{\text{comp}} = \overline{\Omega_{\text{phys}}} \cup \Omega_{\text{PML}}$. To ensure that boundary interactions do not propagate into the physical domain, the coordinate is stretched in the PML

$$\tilde{y} = y + \mathrm{e}^{\mathrm{i}\vartheta_y} \int_{L_y^*}^{y} \sigma(s)\, ds\,, \quad \sigma(s) = 0 \quad \text{if } s \in \Omega_{\text{Phys}}\,.$$

Here $\vartheta_y \in (0, \frac{\pi}{2})$ is a real constant and $\sigma(s)$ is the real-valued absorbing function. This coordinate transform applied to the operator $\mathcal{D} = \mathcal{D}(x, y)$ yields the PML operator

$$\mathcal{D}_{\text{PML}} = k^2 + \frac{1}{S_y}\,\partial_y\Big(\frac{1}{S_y}\partial_y\Big)$$

from the chain rule, where

$$S_y = S_y(y) = \begin{cases} 1\,, & |y| < L_y^*\,, \\ 1 + \mathrm{e}^{\mathrm{i}\vartheta_y}\sigma(|y| - L_y)\,, & L_y^* \le |y| < L_y\,. \end{cases} \tag{1.7}$$

Note here, that the operator remains unmodified inside the physical domain, is only changed by the introduction of dampening in the PML. In case of the time step of SSP, one can now write the operator $\mathcal{X}$ as

$$\mathcal{X}_{\text{PML}} = \frac{k^2 - k_0^2 + S_y^{-1}\partial_y(S_y^{-1}\partial_y)}{k_0^2}\,. \tag{1.8}$$

The use of a classical SSP method, i.e., solving the subproblems (1.6) using finite differences, has already been discussed in the context of radio physics [31]. The PML formulation modifies the differential operator while preserving the structure of the problem as a whole. Next, we will discuss how to incorporate this modified operator into the spectral SSP framework.

2. Spectral SSP Method. The main goal of this work is to develop a spectral version of the SSP marching algorithm, as described by Equations (1.5) and (1.6) in Section 1, which is compatible with PML. The complication in this case consists in the solution of the equations

$$(1 + b_j \mathcal{X}_{\mathrm{PML}}) w_j(y) = u(x, y)\,, y \in [-L, L], \tag{2.1}$$

with periodic boundary conditions imposed at $y = \pm L$ (replacing Equation (1.6) on the infinite interval).

Observe that the differential part of the operator $\mathcal{X}_{\mathrm{PML}}$ in (1.8) can be computed in the Fourier domain separately from the algebraic part by the formula

$$S_y^{-1}\partial_y\big(S_y^{-1}\partial_y u\big) = \mathcal{F}^{-1}\big\{|S_y|^{-2}|\eta|^2\tilde{u} - \mathrm{i}\eta S_y^{-1}\partial_y(S_y^{-1})\tilde{u}\big\}\,,$$

where η denotes the dual variable to y and $\tilde{u} = \tilde{u}(\eta) = \mathcal{F}\{u\}$ is the Fourier-transformed function u. The solution of (2.1) therefore becomes a trivial task in the Fourier domain if $\delta k^2(y) = k^2(y) - k_0^2 = 0$ and $S_y \equiv 1$.

Recently it was shown [56] that for the case of non-homogeneous medium $\delta k^2(y) \neq 0$ (albeit without the PML) a spectral counterpart of the SSP method can be constructed using a truncated Neumann series expansion of the functions $w_j(y)$

$$\begin{aligned} w_j &= \sum_{m=0}^{\infty} \big(-\tilde{b}_j(1 + b_j\partial_y^2)^{-1}\delta k^2\big)^m (1 + b_j\partial_y^2)^{-1} u \\ &\approx \sum_{m=0}^{M} \big(-\tilde{b}_j(1 + b_j\partial_y^2)^{-1}\delta k^2\big)^m (1 + b_j\partial_y^2)^{-1} u\,, \end{aligned}$$

which can be easily computed using a Fourier-domain representation of $(1 + b_j\partial_y^2)^{-1}$. However, this technique cannot easily be generalized to the case of a PML since there does not seem to be a computationally efficient way to evaluate the inverse of $(1 + b_j S_y^{-1}\partial_y(S_y^{-1}\partial_y))$.

The second possible option is to use a Krylov subspace method to solve (1.6) for the weights of the Padé series. Consider the PML subproblems

$$\big(\mathbb{I} + \tilde{b}_j\delta k^2(y) + \tilde{b}_j\mathcal{D}\big)w_j(y) = u(y)\,, \tag{2.2}$$

in which the differential operator $\mathcal{D}$ is defined by

$$\mathcal{D}u = \frac{1}{S_y(y)}\partial_y\Big(\frac{1}{S_y(y)}\partial_y\Big)\,,$$

and $\mathbb{I}$ refers to the identity operator. On the domain $y \in (-L_y, L_y)$, the differential operator $\partial_y u$ can be evaluated in Fourier space

$$\partial_y u(y) = \sum_{j=-\infty}^{\infty} \mathrm{i}\eta_j\,\tilde{u}_j\,\mathrm{e}^{\mathrm{i}\eta_j y}\,,$$

with the discrete Fourier wave numbers $\eta_j = \frac{\pi j}{L_y}$. Let for this $\tilde{u}_j = \int_{-L_y}^{L_y} u(y)\mathrm{e}^{\frac{-\mathrm{i}\pi j}{L_y}y}\,dy$ be jth Fourier coefficient of u. The perturbation of the wave number due to medium effects $\delta k^2 = k_0^2 - k^2$ is treated as a multiplication operator. The pth coefficient of the Padé expansion, divided by the squared reference wave number, is referred to

as $\tilde{b}_p = b_p/k_0^2$. Numerically, the Fourier Series is truncated, introducing a spectral discretization

$$(\partial_y u)_n = \sum_{j=-N/2}^{N/2-1} \mathrm{i}\eta_j \, \tilde{u}_j \, \mathrm{e}^{\mathrm{i}\eta_j y_n} \, .$$

The problem (2.2) can then be solved iteratively using a Krylov subspace method with a suitable initial guess. Suitable options are GMRES [46] and Bi-CGSTAB [54]. In practice, Bi-CGSTAB is easier to use, because it does not require tuning of a restart period for optimal performance and runs slightly faster.

3. Analytical Properties of the PML–SSP Method. In this section, we establish the stability and convergence properties of the *spectral split-step Padé* (SSSP) method combined with a PML. The analysis is performed in a periodic setting that is consistent with the Fourier discretization employed in the numerical scheme. More precisely, we will prove that Padé approximant $R_P(\mathcal{X})$ in (1.5) acting on a Sobolev space $H^2_{\mathrm{per}}(-L, L)$ of periodic functions defined on the interval $y \in [-L, L]$ has spectral radius $\rho(R_P(\mathcal{X})) \leq 1$. On the discrete level this implies the decreasing of the norm at each step of the marching scheme.

For the sake of simplicity let us assume that the reference wave number is purely real, and that the medium is homogeneous, i.e., $k(x, y) = k_0 = \text{const}$. Clearly, this simplification does not substantially affect the properties of the *PML-modified operator* $\mathcal{X}_{\mathrm{PML}}$. In our case the latter reduces to

$$\mathcal{X}_{\mathrm{PML}} = \mathcal{D}u = \frac{1}{k_0^2} \frac{1}{S_y(y)} \frac{d}{dy} \Big(\frac{1}{S_y(y)} \frac{du}{dy} \Big) ,$$

where the stretching function $S_y(y)$ satisfies (1.7) and $\operatorname{Re} S_y(y) \geq 1$, $\operatorname{Im} S_y(y) \geq 0$ in Ω. The remainder of this section is dedicated to the analysis of the properties of the operator $R_P(\mathcal{D})$.

3.1. The poles of the Padé approximant are located on the lower half-plane. In this section we study the properties of the Padé approximant of the function $f(z)$ defined in (1.4). The principal result that we require for investigation of the stability of the marching scheme is that all the poles of the denominator of its $[P/P]$-Padé approximation are located below the real axis.

We start with two preparatory results.

LEMMA 3.1. *The coefficients c_k of the power series expansion $f(z) = \sum_{k=0}^{\infty} c_k z^k$ of the propagator function satisfy the following identity*

$$\sum_{\substack{k+\ell=m, \\ k\geq 0,\, \ell \geq 0}} c_k \, \bar{c}_\ell = \delta_{0m} \, , \tag{3.1}$$

where δ_{ij} denotes the usual Kronecker delta, and the overbar denotes complex conjugation.

Proof. Let us note that the function $f(z)$ is holomorphic on $\Omega = \mathbb{C} \setminus (-\infty, -1]$, and so is the function $\overline{f(\bar{z})}$. For $z \in \mathbb{R} \cap \Omega$ we also have

$$F(z) \equiv f(z)\overline{f(\bar{z})} - 1 = 0 \, .$$

Since the function $F(z)$ defined by the latter equality is also holomorphic on Ω and identically zero on $\mathbb{R}$, it also vanishes for all $z \in \Omega$, hence $f(z)\overline{f(\bar{z})} \equiv 1$ on this domain.

Let us now expand the functions on the left-hand side of the last equality into power series at $z = 0$

$$\Big(\sum_{k=0}^{\infty} c_k z^k\Big)\overline{\Big(\sum_{k=0}^{\infty} c_k \bar{z}^k\Big)} = 1\,.$$

Multiplying and combining the terms with identical powers of z, we arrive at the formula

$$\sum_{m=0}^{\infty}\Big(\sum_{k+\ell=m} c_k\,\bar{c}_\ell\Big) z^m = 1\,,$$

from which the condition in the Lemma statement follows. ∎

Consider now the $[P/P]$-Padé approximant $R_P(z) = T_P(z)/Q_P(z)$ (with $\deg T_P = P$, $\deg Q_P = P$), computed from the first $2P+1$ coefficients c_j of the Taylor series of $f(z)$ at $z = 0$. Note that the coefficients of $T_P(z)$, $Q_P(z)$ are found from the linear system obtained by comparing the terms of the powers $z^0, \dots, z^{2P}$ in the asymptotic equality $Q(z)f(z) - T(z) = O(z^{2P+1})$. Its solution is unique up to a common scalar factor whenever the Hankel determinant $\det(c_{P+i-j})_{i,j=1}^{P}$ is nonzero, cf. [6].

LEMMA 3.2 (Conjugate symmetry). *The numerator and the denominator of the Padé approximant $R_P(z)$ are related by the following formula*

$$Q_P(z) = \overline{T_P(\bar{z})}, \qquad z \in \Omega.$$

In particular, this implies $|R_P(z)| = 1$ for $z \in \mathbb{R} \cap \Omega$.

Proof. Consider the polynomials $\tilde{T}(z) := \overline{Q_P(\bar{z})}$ and $\tilde{Q}(z) := \overline{T_P(\bar{z})}$. Taking the complex conjugate of the defining relation $Q_P f - T_P = O(z^{2P+1})$ and using the equality $\overline{f(\bar{z})} = 1/f(z)$ from the proof of Lemma 3.1, we obtain $\tilde{Q}f - \tilde{T} = O(z^{2P+1})$.

Since $[P/P]$-Padé coefficients are unique up to a constant scalar factor, it can be concluded that

$$\tilde{T} = \lambda T_P \text{ and } \tilde{Q} = \lambda Q_P$$

for some $\lambda \in \mathbb{C}$. Now for $z \in \mathbb{R}$ we have

$$|R_P(z)|^2 = \Big|\frac{T_P(z)}{Q_P(z)}\Big|^2 = \frac{T_P(z)\overline{T_P(z)}}{Q_P\overline{Q_P(z)}} = \frac{T_P(z)\overline{T_P(\bar{z})}}{Q_P\overline{Q_P(\bar{z})}} = \frac{T_P\tilde{Q}}{Q_P\tilde{P}} = 1\,.$$

Finally, normalizing $Q_P(0) = 1$ forces $\lambda = 1$. Hence $Q_P(z) = \overline{T_P(\bar{z})}$. For $y \in \mathbb{R}$ this gives $|R_P(z)| = |T_P(z)|/|Q_P(z)| = 1$. ∎

Conjecture 3.3. For all values of t and P, all zeros z_j of Q_P are located below the real axis, i.e., $Q_P(z_j) = 0$ implies $\mathrm{Im}(z_j) < 0$.

This conjecture can be easily proven analytically for $P \le 4$ by computing the coefficients dependent on t using the matrix method (using symbolic algebra systems). For higher Padé orders, direct computations for a typical range of values $t \in (0.4, 200)$ provide numerical evidence that the roots of Q_P lie below the real axis. The results for $P = 5$ and $P = 9$ are displayed in Figure 1. We note that due to the inherent instability of Taylor-to-Padé computations, higher orders P may exhibit roots with slightly positive imaginary part, as described in Remark 1.1.

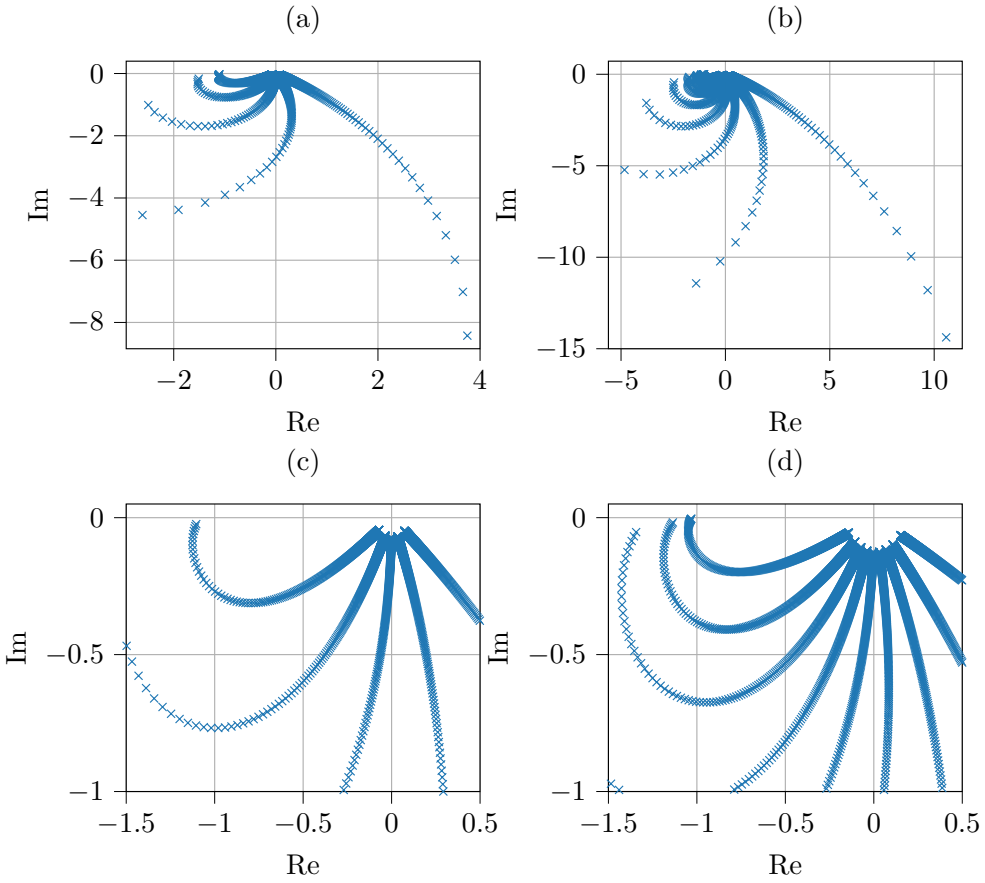

Fig. 1: 500 numerically computed poles of the Padé expansions of (1.4) for both $P = 5$ ((a) and (c)) and $P = 9$ ((b) and (d)) provide justification for Conjecture 3.3. The poles were computed for $t \in [0.4, 0.8, \ldots, 200]$ via the matrix-method. The lower row ((c) and (d)) provides a zoomed-in view for clarity.

PROPOSITION 3.4. *From Conjecture 3.3 it follows that* $|R_P(z)| \leq 1$ *for all* z *such that* $\mathrm{Im}(z) \geq 0$ *with the equality achieved exclusively for* $z \in \mathbb{R}$.

Proof. Assume that $\{z_p\}$, $p = 1, \ldots, P$ are zeros of Q_P. It follows from Lemma 3.2 that $\{\bar{z}_p\}$ are zeros of T_P. Assuming the Conjecture 3.3, we have $\mathrm{Im}(z_p) < 0$ and, accordingly, $\mathrm{Im}(\bar{z}_p) > 0$.

Let us now rewrite R_P in the following way

$$R_P = \varkappa \prod_{p=1}^{P} \frac{z - \bar{z}_p}{z - z_p}\,, \tag{3.2}$$

where $|\varkappa| = 1$ since $|R_P(z)| = 1$, $z \in \mathbb{R}$. Let us explicitly introduce real and imaginary parts of the numbers $z = \xi + \mathrm{i}\eta$ and $z_p = \xi_p + \mathrm{i}\eta_p$. Then the magnitudes of the factors in (3.2) can be estimated as

$$|z - \bar{z}_p|^2 = (\xi - \xi_p)^2 + (\eta + \eta_p)^2\,,$$

$$|z - z_p|^2 = (\xi - \xi_p)^2 + (\eta - \eta_p)^2 .$$

Assuming now $\eta \geq 0$ and recalling that $\eta_j < 0$ we observe that $|\eta - \eta_p|^2 \geq |\eta + \eta_p|^2$, which implies $|z - \bar{z}_p| \leq |z - z_p|$. In other words, each factor in (3.2) satisfies $\left|\frac{z-\bar{z}_p}{z-z_p}\right| \leq 1$, and the equality is fulfilled if and only if $\eta = 0$. ∎

3.2. Sesquilinear Form and the Spectrum of $\mathcal{D}$. In the previous subsection we showed that the poles of the symbol of the propagator's Padé approximation (1.5) are located in the lower half-plane. If we could prove that the spectrum (or, say, numerical range) of the operator $\mathcal{X}$ is restricted to the upper half-plane, the inequality from the Proposition 3.4 would guarantee non-increasing of the norm by the SSP marching scheme (1.5). In order to achieve this objective, we follow roughly the same path as the authors of [27] in our periodic setting.

Let us consider the following non-Hermitian bounded sesquilinear form

$$\langle u, v\rangle_S = \int_{-L}^{L} S(y) u(y) \bar{v}(y)\, dy \tag{3.3}$$

on $H^2_{\mathrm{per}}(-L, L)$ that satisfies the property $\langle u, v\rangle_S = \overline{\langle u, v\rangle}_{\bar{S}}$.

PROPOSITION 3.5. *Every eigenvalue λ of the operator $\mathcal{D}$ defined on $H^2_{\mathrm{per}}(-L, L)$ has the positive imaginary part, i.e.* $\mathrm{Im}(\lambda) \geq 0$.

Proof. Assume that λ is an eigenvalue of $\mathcal{D}$, and $u_\lambda(y)$ its eigenfunction, i.e.,

$$\mathcal{D}u_\lambda = \lambda u_\lambda , \quad u_\lambda \neq 0 .$$

We substitute both sides of this equality into $\langle \cdot, u_\lambda\rangle_S$. On the left-hand side we have

$$\langle \mathcal{D}u_\lambda, u_\lambda\rangle_S = \int_{-L}^{L} S(y)\, \mathcal{D}u_\lambda(y) \bar{u}_\lambda\, dy = \frac{1}{k_0^2} \int_{-L}^{L} \partial_y \Big(\frac{1}{S} \partial_y u_\lambda\Big) \bar{u}_\lambda\, dy$$

$$= \frac{1}{k_0^2} \left[\frac{1}{S} \partial_y u_\lambda \bar{u}_\lambda |_{-L}^{L} - \int_{-L}^{L} \frac{1}{S} \partial_y u_\lambda \partial_y \bar{u}_\lambda\, dy \right] = -\frac{1}{k_0^2} \int_{-L}^{L} \frac{1}{S} |\partial_y u_\lambda|^2\, dy \overset{\text{by def}}{=} \alpha + \mathrm{i}\beta .$$

Observing that $\frac{1}{S} = \frac{1-\mathrm{i}\sigma}{1+\sigma^2}$ (where $\sigma(y)$ is real and non-negative), we conclude that

$$\alpha = -\frac{1}{k_0^2} \int_{-L}^{L} \frac{|\partial_y u_\lambda|^2}{1+\sigma^2} dy \leq 0 , \qquad \beta = \frac{1}{k_0^2} \int_{-L}^{L} \frac{\sigma |\partial_y u_\lambda|^2}{1+\sigma^2} dy \geq 0 .$$

At the same time, on the right-hand side we obtain

$$\langle \lambda u_\lambda, u_\lambda\rangle_S = \lambda \int_{-L}^{L} S|u|^2 dy \overset{\text{by def}}{=} \lambda(\mu + \mathrm{i}\nu) ,$$

where $\mu > 0$, $\nu > 0$. Equality $\langle \mathcal{D}u_\lambda, u_\lambda\rangle_S = \langle \lambda u_\lambda, u_\lambda\rangle_S$ therefore implies that

$$\lambda = \frac{\alpha + \mathrm{i}\beta}{\mu + \mathrm{i}\nu} = \frac{(\alpha + \mathrm{i}\beta)(\mu - \mathrm{i}\nu)}{\mu^2 + \nu^2} .$$

Since both $\mu\beta$ and $-\nu\alpha$ are non-negative, it is clear that $\mathrm{Im}(\lambda) \geq 0$. ∎

3.3. Spectral Radius of $R_P(\mathcal{D})$. To conclude this section, we emphasize that our iterations given by (1.5) transform the functions from $H^2_{\mathrm{per}}(-L, L)$ to the functions from the same space. This fact follows from regularity theorems [19] that are usually formulated for the case of Dirichlet boundary conditions but can be also proven in the periodic case without any substantial reformulation.

3.4. Discrete Fourier Stability. We now investigate the stability of the fully discrete scheme from the perspective of its Fourier representation. Because the spatial discretization is based on a Fourier spectral method, analyzing the behavior of individual Fourier modes is a natural approach. To this end, we express the numerical solution at a fixed range step in terms of its discrete Fourier series,

$$u_N(y) = \sum_{j=-N/2}^{N/2-1} \hat{u}_j \, \mathrm{e}^{\mathrm{i}\eta_j y}, \qquad \eta_j = \frac{\pi j}{L_y}.$$

In this representation, differentiation with respect to y corresponds to a multiplication by $\mathrm{i}\eta_j$, allowing us to interpret the action of the differential operators mode by mode.

Without a PML, the second derivative operator acts diagonally in Fourier space, with eigenvalues $-\kappa_j^2$. The presence of the PML modifies this structure via the complex stretching function $S_y(y)$. This formally leads to a modified symbol of the form $-\kappa_j^2/S_y^2(y)$, which introduces a complex-valued damping factor. Since $\operatorname{Re} S_y(y) \geq 1$ and $\operatorname{Im} S_y(y) \geq 0$, the real part of this expression is non-positive, indicating that the PML induces attenuation of the Fourier modes, particularly for large wave numbers.

Combining this with the bounded contribution of the wave number term $k^2(y)$, we obtain an effective symbol for the operator $\mathcal{X}_{\mathrm{PML}}$ of the form

$$\lambda_j(y) = \frac{k^2(y) - k_0^2 - \eta_j^2/S_y^2(y)}{k_0^2}.$$

The behavior of the numerical scheme can thus be understood by examining how each mode propagates under the Padé approximation.

For a single propagation step, each Fourier mode is multiplied by an amplification factor of the form

$$G_j = \mathrm{e}^{\mathrm{i}k_0 h}\left(d_0 + \sum_{j=1}^{P} \frac{d_j}{1 + b_j\lambda_p}\right).$$

The exponential prefactor has unit modulus and therefore does not affect stability. The remaining expression depends on the location of λ_p in the complex plane.

As discussed earlier, the real part of λ_p is bounded due to the dissipative contribution of the PML. Specifically, the damping term $-\eta_j^2/S_y^2(y)$ shifts high-frequency modes further into the stable region of the complex plane. Since the Padé coefficients satisfy $\operatorname{Re} b_p > 0$, the denominators $1 + b_p\lambda_p$ remain bounded away from zero, and the amplification factor remains finite.

This implies that the magnitude of G_p does not grow uncontrollably with p. More precisely, there exists a constant C such that $|G_p| \leq 1 + Ch$, uniformly in p and N, for sufficiently small step size h. Thus, the discrete solution satisfies the stability bound

$$\|u_N^{n+1}\|_{\ell^2} \leq (1 + Ch)\,\|u_N^n\|_{\ell^2},$$

where the norm is defined via the Fourier coefficients.

We observe that the presence of the PML stabilizes the scheme by introducing additional damping for high-frequency components. This prevents the accumulation of unresolved oscillations, thereby contributing to the robustness of the method in practical computations.

4. Radiowave Propagation in the Troposphere. Wide-angle parabolic equations based on the Padé expansion of an operator square root exponential appear in the literature in several different contexts. In the first example, we address the problem of tropospheric radiowave propagation. In this case, equation is solved on a vertical half-plane (x, z coordinates, z is the altitude, $z = 0$ is the Earth's surface).

4.1. The Problem Statement. In two-dimensional Cartesian coordinates, the horizontally polarized, time-harmonic (monochromatic) electric field component $E_y(x, z) = \psi(x, z)$ can be described by the 2D Helmholtz equation

$$\partial_x^2\psi + \partial_z^2\psi + k_0^2 m^2 \psi = \delta(x)Q(z)\,, \tag{4.1}$$

where k_0 is the wave number of the vacuum, and $m^2(x, z) = 1 + 2n(x, z) + 2z/R$. Here, $n(x, z)$ is the variable refractive index, R is the curvature radius of the Earth's surface, and $Q(z)$ models the geometry of the antenna. This problem setup is very common across the radio physics community [30, 41, 39, 40].

Assuming that back-scattering in the horizontal direction is negligible, one can replace the BVP for (4.1) by a Cauchy problem for its one-way counterpart

$$\partial_x u = \mathrm{i}k\big(\sqrt{1+\mathcal{X}} - 1\big)u\,, \quad u|_{x=0} = u_0(z)\,,$$

where $u(x, z) = \mathrm{e}^{-\mathrm{i}k_0 x}\psi(x, z)$ is an envelope function of a rapidly oscillating electric field, and the Cauchy data $u_0(z)$ is defined through $Q(z)$.

The ground can be represented by a homogeneous Dirichlet boundary condition. Due to changes in the refractive index, the radio field is usually partially reflected at the boundary between atmospheric layers. The rest of the field then escapes into the higher layers of the atmosphere. Efficient simulation requires one-sided truncation of the domain, which was achieved using a PML. In this scenario, homogeneous Dirichlet boundary conditions can be addressed by extending the domain with a mirror domain, as described by Smith and Tappert [48].

4.2. Numerical Results. The computation is an example of a radio wave with a frequency of 300 MHz emitted from a parabolic antenna and propagating through the lower atmosphere. We use the initial condition is modeled as

$$u_0(z) = \frac{k_0\beta}{2\pi\log_{10}(2)}\,\mathrm{e}^{-\mathrm{i}k_0\theta_0 z}\,\mathrm{e}^{-\frac{\beta^2 k_0^2}{8\log_{10}(2)}(z-z_0)},$$

with $\beta = 10°$, $\theta_0 = 10°$ and $k_0 = \frac{\omega}{c_0} = 2\pi\,\mathrm{m}^{-1}$. The modified refractive index is defined via

$$m^2(z) = \begin{cases} z/250 - 1/2 & \text{if } z \in [0, 100] \\ 0 & \text{else} \end{cases}.$$

This setting was chosen to show the method's capability to reproduce reflections caused by discontinuities in the equations coefficients representing media interfaces. A PML with a width of 10 meters was used above $z = 200\,\mathrm{m}$. Both the spectral as

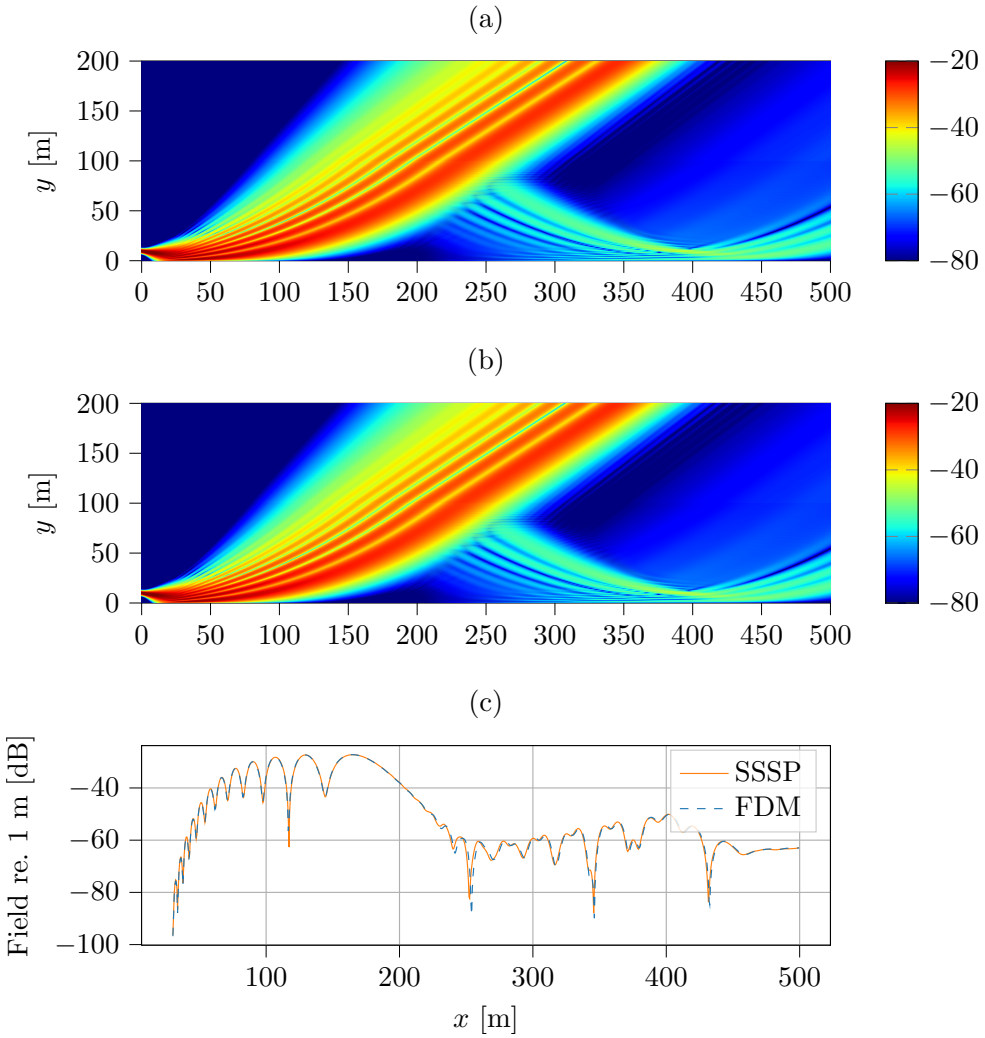

Fig. 2: Radio wave propagation. (a) shows a reference field computed by Finite Difference SSP, (b) shows the field computed by SSSP and (c) shows a comparison along a slice at $z = 30\,\mathrm{m}$. All fields are displayed in dB re. 1 m.

well as the finite difference method were run for $P = 1$ with the step size of 0.1 m in x as well as 2048 points in z. For the SSSP simulation, BiCGStab was employed to solve the system, using a multiplicative preconditioner $\mathcal{X}_0^{-1} = (1 + k_0^2 n^2)^{-1}(1 + \partial_y^2)^{-1}$ and a relative tolerance of 10^{-6} as stopping criterion.

The radio signal gets focused into the upper atmosphere by the gradient in the refractive index in the lower troposphere. The discontinuity at $z = 100\,\mathrm{m}$ introduces reflections of the field back towards the Earth's surface $z = 0$.

As shown in Fig. 2, the SSSP solution is in excellent agreement well with the finite difference SSP, even at comparably small number of points in z.

5. Sound Propagation in a 3D Shallow-Water Waveguide. The second case is related to the propagation of acoustic waves in a three-dimensional shallow water environment. This problem can be reduced to solving several one-way counterparts of the 2D Helmholtz equation within the framework of adiabatic normal modes [26, 43]. A domain truncation issue naturally arises because the area of interest is typically a small part of the ocean, and reflection-free transmission through its boundaries is essential in practical problems.

5.1. Mode Parabolic Equations. We consider the stationary acoustic field $p = p(x, y, z)$ produced by a time-harmonic point source of the frequency f is located at $x = 0, y = 0, z = z_s$, that can be described by the *three-dimensional Helmholtz equation* [26]

$$\begin{aligned} &\partial_x^2 p + \partial_y^2 p + \partial_z^2 p + \frac{\omega^2}{c^2}\, p = -\delta(x, y, z - z_s), \quad \text{in } \Omega\,, \\ &p|_{z=H} = 0\,, \quad p|_{z=0} = 0\,, \end{aligned} \tag{5.1}$$

in the domain $\Omega = (-\infty, \infty) \times (-\infty, \infty) \times [0, H]$, where $z = 0$ is the sea surface, $z = H$ is lower boundary of computational domain (typically taken to be sufficiently large in order to incorporate one or several layers of sediments). It is also assumed that a suitable Sveshnikov-type radiation boundary condition is imposed for $r = \sqrt{x^2 + y^2} \to \infty$ in order to guarantee uniqueness of the solution of Eq. (5.1) (see, e.g., [33]). Here, $\omega = 2\pi f$ is the angular frequency, and $c(x, y, z)$ denotes the speed of sound.

One then employs the *modal expansion ansatz*

$$p(x, y, z) = \sum_{j=1}^{N_m} \mathcal{A}_j(x, y)\, \phi_j(z; x, y)\,, \tag{5.2}$$

where $\phi_j(z; x, y)$ are mode functions computed from the media parameters at the point (x, y), and $\mathcal{A}_j(x, y)$ are the corresponding mode amplitudes.

Under adiabatic assumption it can be shown [26] mode amplitudes satisfy a two-dimensional Helmholtz equation

$$\partial_x^2 \mathcal{A}_j + \partial_y^2 \mathcal{A}_j + k_j^2 \mathcal{A}_j = -\delta(x)\delta(y) \frac{\phi_j(z_s)}{\rho_w}\,. \tag{5.3}$$

The one-way counterpart of Eq. (5.3) is called pseudodifferential *mode parabolic equation* (MPE)

$$\partial_x \mathcal{A}_j = \mathrm{i}\sqrt{\partial_y^2 + k_j^2}\, \mathcal{A}_j\,, \quad x, y \in (0, x_{\max}) \times (-L_y^*, L_y^*)\,, \tag{5.4}$$

which identical to Eq. (1.2).

It has been shown recently that SSP method is particularly efficient for solving Eq. (5.4) [43, 44] as was already mentioned in Sec. 1. In this section we that its spectral counterpart is also excels in this task.

5.2. Test scenarios. In the framework of the mode parabolic equations theory, we consider two scenarios of sound propagation in shallow water.

First, we examine a Pekeris-type waveguide with a flat bottom to verify the capabilities of the PML (see Fig. 3a). Then, we address the classic issue of sound propagation in a coastal wedge [26], i.e., a shallow sea with a sloping bottom (see Fig. 3b). In

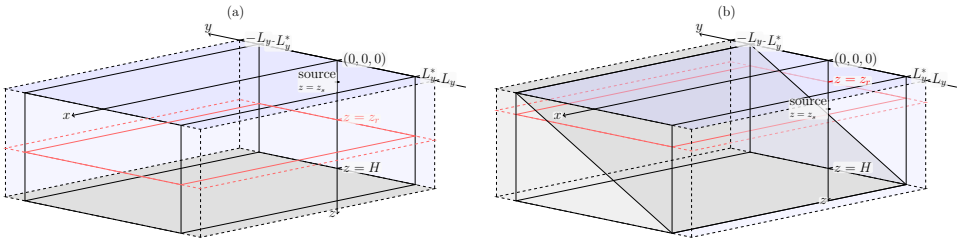

Fig. 3: The domains of the mode parabolic equation in underwater acoustics. The dashed box contains the computational domain $\Omega_{\text{comp}} = (0, R) \times (-L_y^*, L_y^*) \times (0, H)$ consisting of the physical domain $\Omega_{\text{phys}} = (0, R) \times (-L_y^*, L_y^*) \times (0, H)$ represented by the continuously drawn box and a perfectly matched absorbing layer in y. An initial impulse emitted by the source at $(0, 0, z_s)$ is propagated in x direction. The results are presented at the plane $z = z_r$, shown in red. (a) displays the general setting, while (b) shows the specific wedge test case, with the bottom slope across the propagation direction x.

both scenarios, our waveguide consists of an upper layer representing seawater (with a sound speed of $c = 1500\,\text{m/s}$ and a density $\rho = 1\,\text{g/cm}^3$) and a bottom sediment (sound speed $c = 1700\,\text{m/s}$, density $\rho = 1.5\,\text{g/cm}^3$). The computational domain is chosen as $\Omega_{\text{phys}} = \{(x, y, z) | 0 \le x \le 25\,\text{km},\ -4\,\text{km} \le y \le 4\,\text{km},\ 0 \le z \le 400\,\text{m}\}$. The acoustic field $p(x, y, z)$ is computed using Eq. (5.2), and the normal modes $\phi_j(z, x, y)$ and their wavenumbers $k_j(x, y)$ are obtained using the `ac_modes` solver [43]. The proposed SSSP method is then used to solve equations (5.4) with initial conditions $\mathcal{A}_j(0, y)$, which are obtained using the so-called ray starter [43]. 400 m-wide PMLs are added on both sides of the domain (at $y = \pm L_y^*$).

In both cases, we compute the acoustic field due to a point source of the frequency $f = 25\,\text{Hz}$, located at $z_s = 100\,\text{m}$, $y_s = 0\,\text{m}$, $x_s = 0\,\text{m}$. We compare and visualize the computational results for the horizontal plane $z = z_r = 30\,\text{m}$. A [9/9]-Padé approximation is used in both cases, and $N_m = 8$ modes are taken into account.

To solve the linear system for all numerical simulations, the BiCGStab method used a multiplicative preconditioner $\mathcal{X}_0^{-1} = (1 + \delta k^2)^{-1}(1 + \partial_y^2)^{-1}$. The method was run up to a relative tolerance of 10^{-8}, though higher tolerances yield accurate results, both qualitatively and quantitatively.

5.2.1. Flat Bottom. In the first numerical experiment acoustic field is computed for a shallow-water Pekeris waveguide, displayed with the constant water depth of $h_b = 200\,\text{m}$ (i.e., with flat horizontal bottom, see Fig. 3a). The domain was discretized into 512 points in y, corresponding to the mesh size 17.187 m, or a bit less than 4 points per wavelength and into 500 points in x, corresponding to the step size $h = 50\,\text{m}$.

The resulting acoustic field at exhibiting a typical circular interference pattern is displayed in Fig. 4 (we do not present reference solution, but it ideally coincides with the one obtained using SSSP). Note that the utilized discretization step in y is coarser than a finite difference method permits [44].

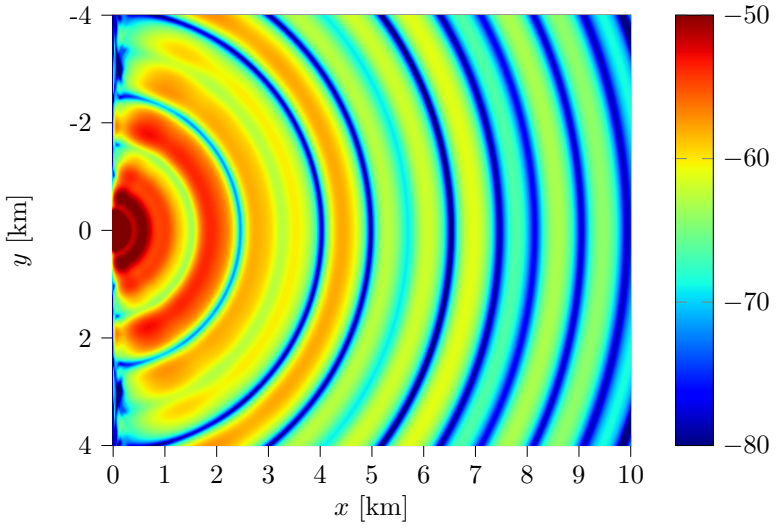

Fig. 4: Acoustic pressure in dB re 1 m at $z_r = 30$ m in the Pekeris waveguide.

5.2.2. Wedge. In the coastal wedge benchmark problem [26] the water depth is a function of y:

$$h_b = h_b(y) = h_{b,0} + \tan(\alpha) y \,,$$

where $h_{b,0} = 200$ m, and the bottom slope angle is $\alpha \approx 2.86°$.

A step size of 50 m was used again, and to demonstrate numerical convergence of the discretization in y, the resulting fields are displayed for 512 and 4096 y points, corresponding to discretization constants of 17.1875 m and ~ 2.15 m, respectively.

The acoustic field in the wedge exhibits a remarkably different interference pattern due to the horizontal refraction effect, which causes acoustic energy to propagate towards the deeper part of the sea area. Consequently, the field is no longer symmetric with respect to the x-axis, as shown in Fig. 5. In particular, the water-borne modes experience a cutoff around $z \approx 30$, thus producing a silent zone near the coast. The displayed fields agree qualitatively and quantitatively with the reference solution by the source image method [15], as shown in Fig. 5c, even when a coarse grid is used.

Despite not considering mode interactions, the SSSP method produces a highly accurate field with a small number of discretization points.

6. Conclusion. This study presents a spectral SSP algorithm for wave propagation modeling problems in the frequency domain. This marching numerical scheme integrates one-way counterparts of the Helmholtz equation, though it can be used for other elliptic problems, such as Lamé equations in elasticity theory or a coupled system of equations for normal mode amplitudes. The novelty of the proposed method consists in the fact that it uses a spectral representation (via FFT) to compute derivatives, whereas standard SSP-based solvers use finite differences for this purpose. In the presence of perfectly matched layers, the inversion of the transverse differential operator is accomplished using the iterative Bi-CGSTAB method. Although similar

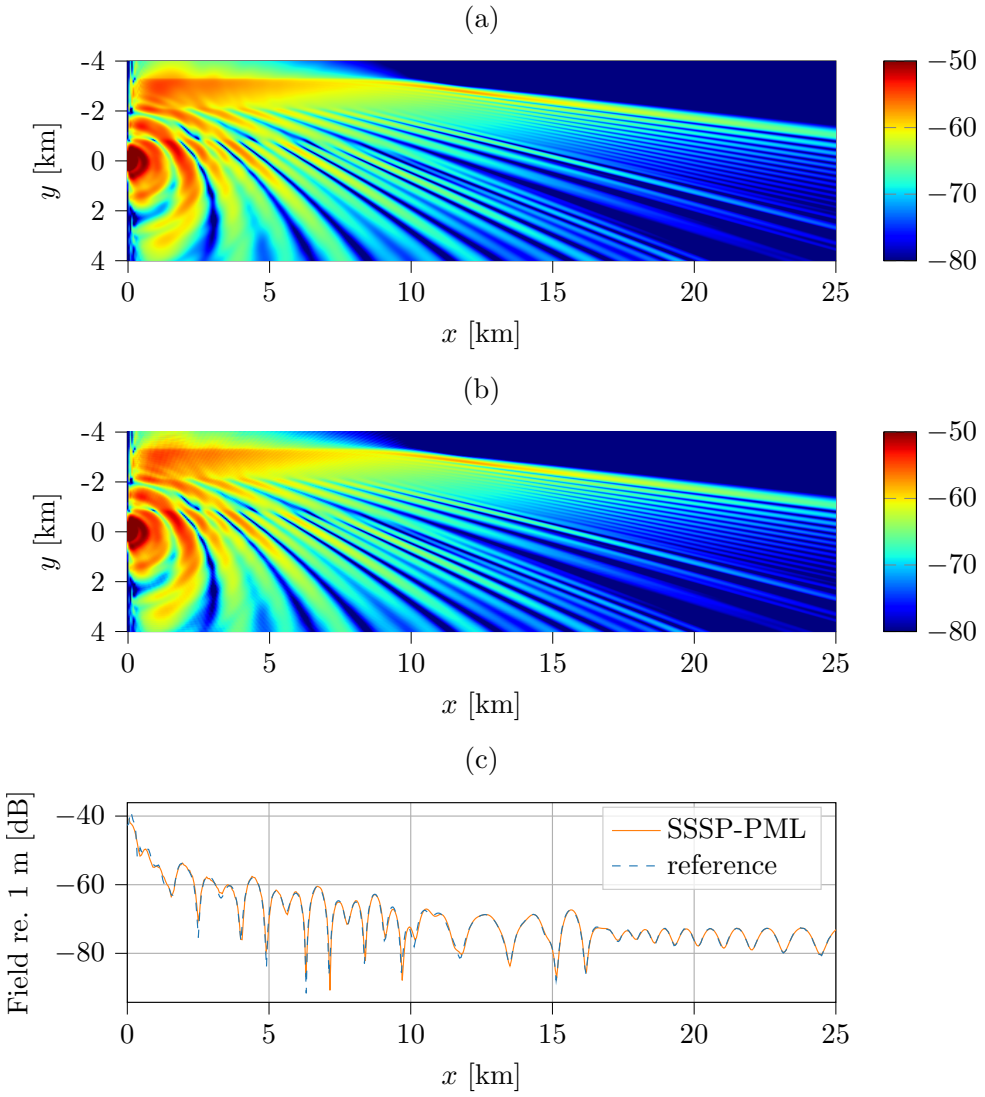

Fig. 5: Acoustic field (in dB re 1 m) in the wedge at $z_r = 30\,\mathrm{m}$. (a) using 4096 points along y, (b) only using 512 points along y and (c) comparing the field (b) with the method of source images.

approaches have been proposed in the literature for certain classes of PDEs [2, 3], SSSP method proposed here is the first one to deal with a pseudodifferential equation (1.4). The capabilities of the developed approach are demonstrated through two examples of realistic propagation scenarios from underwater acoustics and radiowave theory (see the GitLab repository https://git.uni-wuppertal.de/walsken/sssp-pml).

Theoretically, evaluating one Padé term w_j, is of order $O(N)$. For example, the second-order finite-difference approximation of the transverse operator $\mathcal{X}$ requires $O(N \log(N))$ operations, whereas evaluating one Padé term requires only $O(N)$. Thus,

one might question the pursuit of making the SSP method spectral. However, this superficial complexity estimate applies only to traditional multi-core or single-core architectures based on serial CPUs. In the context of highly parallel computing systems, including modern GPUs and FPGAs, FFT libraries that are optimized to use massive concurrent threads can easily outperform traditional sequential algorithms for sparse matrix inversion. At the same time, the spectral accuracy of the derivative approximation within the SSSP method allows one to achieve lower computational errors with fewer discretization points, as shown in [56], especially in cases of continuous variation of the media parameters. This is particularly evident in mode parabolic equations in underwater acoustics, where the ocean environment typically exhibits slow and smooth variations in the x and y dimensions. The situation differs when a wide-angle parabolic equation is solved in the vertical plane (i.e., in the x and z coordinates). Although media parameters are expected to vary slowly in deep-water propagation scenarios, finite differences are much more practical in shallow-water geoacoustic waveguides with multiple interfaces where sound velocity has discontinuities. Thus, the presented approach could excel in specific problem classes and computational architectures rather than being a jack of all trades.

On the other hand, we find that the question of whether SSP can be combined with spectral discretization in some way is also of theoretical interest, at least. In our opinion, this study provides a positive answer.

A promising direction for future work is developing quantum-compatible variants of the proposed spectral split-step Padé (SSSP) framework. The exponential propagator underlying the method is structurally analogous to quantum time evolution and can be approximated using operator-splitting techniques, such as Trotter-Suzuki decompositions [50] or modern Hamiltonian simulation methods [35]. In particular, the separation into Fourier-diagonal and multiplicative operators naturally aligns with quantum algorithms based on the quantum Fourier transform and the linear combination of unitaries approach [9]. However, a key challenge remains: the treatment of the non-Hermitian PML operator would require extensions to open-system quantum simulation frameworks [28].

REFERENCES

[1] A. T. Abawi, W. A. Kuperman, and M. D. Collins. The coupled mode parabolic equation. *J. Acoust. Soc. Am.*, 102(1):233–238, 1997.
[2] X. Antoine, F. Fillion-Gourdeau, E. Lorin, and S. MacLean. Pseudospectral computational methods for the time-dependent Dirac equation in static curved spaces. *J. Comput. Phys.*, 411:109412, 2020.
[3] X. Antoine and X. Zhao. Pseudospectral methods with PML for nonlinear Klein-Gordon equations in classical and non-relativistic regimes. *J. Comput. Phys.*, 448:110728, 2022.
[4] D. Appelö, Th. Hagstrom, and G. Kreiss. Perfectly matched layers for hyperbolic systems: general formulation, well-posedness, and stability. *SIAM J. Appl. Math.*, 67(1):1–23, 2006.
[5] V. Avilov. Pseudodifferential parabolic equations of sound propagation in the slowly range-dependent ocean and its numerical solution. *Acoust. Phys.*, 41:1–7, 1995.
[6] G. A. Baker and P. Graves-Morris. *Padé Approximants*. Encyclopedia of Mathematics and its Applications. Cambridge University Press, 2nd edition, 1996.
[7] E. Bécache, P. Joly, and C. Tsogka. An analysis of new mixed finite elements for the approximation of wave propagation problems. *SIAM J. Numer. Anal.*, 37(4):1053–1084, 2000.
[8] J.-P. Berenger. A perfectly matched layer for the absorption of electromagnetic waves. *J. Comput. Phys.*, 114(2):185–200, 1994.
[9] D. W. Berry, G. Ahokas, R. Cleve, and B. C. Sanders. Efficient quantum algorithms for simulating sparse Hamiltonians. *Commun. Math. Phys.*, 270(2):359–371, 2007.
[10] J. P. Boyd. *Chebyshev and Fourier Spectral Methods*. Courier Corporation, 2001.
[11] W. C. Chew and W. H. Weedon. A 3D perfectly matched medium from modified Maxwell's

equations with stretched coordinates. *Microwave Opt. Techn. Lett.*, 7(13):599–604, 1994.
[12] J. F. Claerbout. *Fundamentals of geophysical data processing with application to petroleum prospect*. McGraw-Hill, 1976.
[13] M. D. Collins. A split-step Padé solution for the parabolic equation method. *J. Acoust. Soc. Am.*, 93(4):1736–1742, 1993.
[14] M. D. Collins and W. L. Siegmann. *Parabolic Wave Equations with Applications*. Springer, 2019.
[15] G. B. Deane and M. J. Buckingham. An analysis of the three-dimensional sound field in a penetrable wedge with a stratified fluid or elastic basement. *J. Acoust. Soc. Am.*, 93(3):1319–1328, 1993.
[16] A. Dedner, D. Kröner, I. L. Sofronov, and M. Wesenberg. Transparent boundary conditions for MHD simulations in stratified atmospheres. *J. Comput. Phys.*, 171(2):448–478, 2001.
[17] A. Dronamraju, S. Li, Q. Li, Y. Li, D. Tylavsky, D. Shi, and Z. Wang. Implications of Stahl's theorems to holomorphic embedding part II: Numerical convergence. *CSEE J. Power Energy Syst.*, 7(4):773–784, 2021.
[18] M. Ehrhardt, J. Glück, P. Petrov, and S. Tappe. Square root operators and the well-posedness of pseudodifferential parabolic models of wave phenomena. *Appl. Math. Lett.*, page 109644, 2025.
[19] L. C. Evans. *Partial differential equations*, volume 19. American Mathematical Society, 2022.
[20] M. D. Feit and J. A. Fleck Jr. Light propagation in graded-index optical fibers. *Applied Optics*, 17(24):3990–3998, 1978.
[21] D. Givoli. *Numerical methods for problems in infinite domains*, volume 33 of *Studies in Applied Mechanics*. Elsevier, 2013.
[22] O. A. Godin. Reciprocity and energy conservation within the parabolic approximation. *Wave Motion*, 29(2):175–194, 1999.
[23] P. Gonnet, S. Güttel, and L. N. Trefethen. Robust Padé approximation via SVD. *SIAM Review*, 55(1):101–117, 2013.
[24] Th. Hagstrom. Radiation boundary conditions for the numerical simulation of waves. *Acta Numerica*, 8:47–106, 1999.
[25] J. S. Hesthaven. On the analysis and construction of perfectly matched layers for the linearized Euler equations. *J. Comput. Phys.*, 142(1):129–147, 1998.
[26] F. B. Jensen, W. A. Kuperman, M. B. Porter, H. Schmidt, and A. Tolstoy. *Computational Ocean Acoustics*, volume 2011. Springer, 2011.
[27] S. Kim and J. E. Pasciak. Analysis of the spectrum of a Cartesian perfectly matched layer (PML) approximation to acoustic scattering problems. *J. Math. Anal. Appl.*, 361(2):420–430, 2010.
[28] N. Kushida and Y.-T. Lin. A quantum computing framework for finite-difference time domain and parabolic equation models in ocean acoustics. In *Proceedings of Meetings on Acoustics*, volume 60, page 022003. Acoustical Society of America, 2025.
[29] M. A. Leontovich and V. A. Fock. Solution of the problem of electromagnetic wave propagation along the Earth's surface by the method of parabolic equation. *J. Phys. USSR*, 10:13–23, 1946.
[30] M. Levy. *Parabolic equation methods for electromagnetic wave propagation*. The Institution of Engineering and Technology, 2000.
[31] M. F. Levy. Perfectly matched layer truncation for parabolic wave equation models. *Proc. Royal Soc. London. A: Math. Phys. Engrg. Sci.*, 457(2015):2609–2624, 2001.
[32] Y.-T. Lin, T. F. Duda, and A.E. Newhall. Three-dimensional sound propagation models using the parabolic-equation approximation and the split-step Fourier method. *J. Comput. Acoust.*, 21(01):1250018, 2013.
[33] Lihan Liu, Yuehai Qin, Yongzhi Xu, and Yuqiu Zhao. The uniqueness and existence of solutions for the 3-d helmholtz equation in a stratified medium with unbounded perturbation. *Mathematical Methods in the Applied Sciences*, 36(15):2033–2047, 2013.
[34] Q.-H. Liu and J. Tao. The perfectly matched layer for acoustic waves in absorptive media. *J. Acoust. Soc. Am.*, 102(4):2072–2082, 1997.
[35] S. Lloyd. Universal quantum simulators. *Science*, 273(5278):1073–1078, 1996.
[36] Y. Y. Lu. One-way large range step methods for Helmholtz waveguides. *J. Comput. Phys.*, 152(1):231–250, 1999.
[37] Y. Y. Lu. Improving beam propagation method for TM polarization. *Opt. Quant. Electr.*, 35(4):507–519, 2003.
[38] Y. Y. Lu. Some techniques for computing wave propagation in optical waveguides. *Commun. Comput. Phys.*, 1(6):1056–1075, 2006.
[39] M. S. Lytaev. Nonlocal boundary conditions for split-step Padé approximations of the Helm-

holtz equation with modified refractive index. *IEEE Antennas Wireless Prop. Lett.*, 17(8):1561–1565, 2018.

[40] M. S. Lytaev. Numerical method-informed deeponet for refractivity inversion in waveguides. *J. Comput. Sci.*, page 102788, 2026.

[41] M. S. Lytaev and A. G. Vladyko. Split-step Padé approximations of the Helmholtz equation for radio coverage prediction over irregular terrain. In *2018 Advances in Wireless and Optical Communications (RTUWO)*, pages 179–184, 2018.

[42] P. S. Petrov, M. Ehrhardt, and S. B. Kozitskiy. A generalization of the split-step Padé method to the case of coupled acoustic modes equation in a 3D waveguide. *J. Sound Vibr.*, 577:118304, 2024.

[43] P. S. Petrov, M. Ehrhardt, A. G. Tyshchenko, and P. N. Petrov. Wide-angle mode parabolic equations for the modelling of horizontal refraction in underwater acoustics and their numerical solution on unbounded domains. *J. Sound Vibr.*, 484:115526, 2020.

[44] P.S. Petrov and X. Antoine. Pseudodifferential adiabatic mode parabolic equations in curvilinear coordinates and their numerical solution. *J. Comput. Phys.*, 410:109392, 2020.

[45] A. V. Popov and S. A. Hozioskii. A generalization of the parabolic equation of diffraction theory. *Zh. Vychisl. Mat. Mat. Fiz.*, 17(2):527–533, 1977.

[46] Y. Saad and M. H. Schultz. GMRES: A generalized minimal residual algorithm for solving nonsymmetric linear systems. *SIAM J. Sci. Stat. Comput.*, 7(3):856–869, 1986.

[47] J. Shen and L.-L. Wang. Some recent advances on spectral methods for unbounded domains. *Commun. Comput. Phys.*, 5(2-4):195–241, 2009.

[48] K. B. Smith and F. D. Tappert. UMPE: the University of Miami parabolic equation model. Version 1.1. Technical report, University of Miami, 1993. `https://oalib-acoustics.org/website_resources/PE/UMPE/UMPE.pdf`.

[49] A. Sommerfeld. Die Greensche Funktion der Schwingungsgleichung. *Jahresbericht der Deutschen Mathematiker-Vereinigung*, 21:309–352, 1912.

[50] M. Suzuki. General theory of higher-order decomposition of exponential operators and symplectic integrators. *Phys. Lett. A*, 165(5-6):387–395, 1992.

[51] L. N. Trefethen. *Spectral Methods in MATLAB*. SIAM, 2000.

[52] L. N. Trefethen and D. Bau. *Numerical Linear Algebra*. Society for Industrial and Applied Mathematics, Philadelphia, PA, 1997.

[53] S. V. Tsynkov. Numerical solution of problems on unbounded domains. a review. *Appl. Numer. Math.*, 27(4):465–532, 1998. Special Issue on Absorbing Boundary Conditions.

[54] H. A. van der Vorst. Bi-CGSTAB: A fast and smoothly converging variant of Bi-CG for the solution of nonsymmetric linear systems. *SIAM J. Sci. Stat. Comput.*, 13(2):631–644, 1992.

[55] S. N. Vlasov and V. I. Talanov. The parabolic equation in the theory of wave propagation: On the 50th anniversary of its publication. *Radiophys. Quant. Electron.*, 38:1–12, 1995.

[56] D. Walsken, P. Petrov, and M. Ehrhardt. A novel Fourier-based split-step Padé method for accurate acoustic field propagation. *Adv. Appl. Math. Mech.*, 18:1602–1615, 2026.

[57] X. Wu, Z. Li, Z. Liang, and Y. Long. Higher order FD-Padé scheme for 3-D parabolic equation in radio-wave propagation. *IEEE Antennas Wireless Prop. Lett.*, 22(6):1251–1255, 2023.